Measurement and analysis of atmospheric optical turbulence in a near-maritime environment

IOP SciNotes

ARTICLE

Measurement and analysis of atmospheric optical turbulence in a near-maritime environment

Christopher Jellen[1], **Charles Nelson**[2], **Cody Brownell**[1], **John Burkhardt**[1] **and Miles Oakley**[2]

[1] Mechanical Engineering Department, United States Naval Academy, Annapolis, MD, 21402, United States of America
[2] Electrical and Computer Engineering Department, United States Naval Academy, Annapolis, MD, 21402, United States of America

E-mail: contact.cdjellen@gmail.com

Keywords: optical turbulence, near-maritime, littoral, Scintillometry, C_n^2

OPEN ACCESS

RECEIVED
5 August 2020

REVISED
4 September 2020

ACCEPTED FOR PUBLICATION
21 September 2020

PUBLISHED
30 September 2020

Abstract

The index of refraction structure constant, C_n^2, characterizing the intensity of optical turbulence, describes the disruption of a propagating electromagnetic beam passing through an inhomogeneously heated turbulent environment. In order to improve predictive models, it is critical to develop a deeper understanding of the relationships between environmental parameters and optical turbulence. To that end, an overwater, 890 m scintillometer link was established along the Chesapeake Bay adjacent to the Severn River in Annapolis, Maryland. Specifically, C_n^2 data from the scintillometer, as well, as numerous meteorological parameters were collected over the period of approximately 15 months to characterize a scintillometer link in the near-maritime environment. The characteristics of this near-maritime link were distinct from those observed in prior over-land and open ocean links. Further, existing macro-meteorological models for predicting C_n^2 from environmental parameters developed for open-ocean links were shown to perform poorly in the near-maritime environment. While the offshore adapted macro-meteorological model demonstrated lower prediction error, this study suggests that new models could be developed to reduce C_n^2 prediction error in the near-maritime environment. The complete data set, including C_n^2 measurements, and to our knowledge, one of the first to extend beyond one year, is available.

1. Introduction

Turbulent mixing within the atmosphere causes rapid fluctuations in the local index of refraction resulting in optical turbulence. The intensity of this phenomenon is quantified by the index of refraction structure constant, C_n^2. The magnitude of C_n^2 is directly related to the turbulent structure of the atmosphere which depends on both large-scale atmospheric forcing and on local environmental conditions. At low altitudes, optical turbulence is caused predominantly by temperature gradients within the air [1–3]. Local environmental conditions have been shown to have significant influence [4–6]. Environmental parameters of known importance include humidity and wind speed which are also known to impact the turbulent structure of the air [1–3, 6].

When a laser beam propagates along a path, the fluctuations in the local refractive index result in beam perturbations. These atmospheric effects can lower the energy received at a target or cause information loss in laser communication [1–3]. A deeper understanding of the effect of local conditions on optical turbulence, as quantified by C_n^2, can be applied to improve the accuracy of existing models developed to predict atmospheric effects on beam propagation. The degradation in laser beam quality and the resulting degradation in system performance can be estimated directly from predicted C_n^2. To better inform models for C_n^2 in the near-maritime environment, measurements of a wide range of environmental parameters were collected. This data set can be used to study the accuracy of current models, and to develop new models for the near-maritime environment.

2. Background

Optical turbulence is quantified through the index of refraction structure constant C_n^2, which is a measure of the intensity of the local refractive index fluctuations. The structure function of the refractive index is often calculated using the temperature structure function for the local atmosphere. Path invariance is assumed in the temperature structure function, allowing for approximation of the temperature structure parameter, C_T^2, using point measurements of temperature and pressure. Approximations for the temperature structure function are made through temperature measurement of both large-scale and small-scale eddies along the propagation path. In a near-maritime environment small scale eddies are typically on the order of 1–2 [mm] across, while large scale eddies are on the order of 1–2 [m] across [1, 2]. In general, field measurements of large-scale and small-scale eddies are difficult to collect, and are computed through the use of similarity theory.

Similarity theories employ the use of mean flow characteristics along the propagation path. Monin–Obukhov similarity (MOS) theory is used to describe atmospheric flow behavior for C_n^2 prediction [1, 7, 8]. By assuming parameters such as temperature, humidity, and wind speed are path-invariant, MOS theory can be used to predict mean measurements. Using MOS theory, C_n^2 is predicted using a combination of temperature and humidity effects [1, 7, 8].

While these assumptions simplify the process of predicting C_T^2, and thereby C_n^2, they could also contribute to the generally high, C_n^2, prediction errors observed in the near-maritime environment when using explicit models [9].

In order to support modeling efforts, the refractive index structure parameter C_n^2 is measured in a variety of environments [3–5, 7, 10–12]. The refractive index structure parameter can be determined experimentally by measuring the variance in beam irradiance at a distant target. These irradiance variances are then normalized to compute the scintillation index σ_I^2, defined in equation (1) [1, 2, 7, 9–11].

$$\sigma_I^2 = \frac{\langle \boldsymbol{I}^2 \rangle - \langle \boldsymbol{I} \rangle^2}{\langle \boldsymbol{I} \rangle^2} \tag{1}$$

The scintillation index in equation (1) is a path-dependent measurement of the normalized variance in irradiance along a propagation path. I is the irradiance of the beam at the target at a given time. The brackets in equation (1) denote ensemble averaging [1–3, 11]. The scintillation index σ_I^2 is then used to calculate C_n^2 using the relationship in equation (2) [1, 2, 9, 11].

$$\sigma_I^2 = 1.23 C_n^2 k^{\frac{7}{6}} L^{\frac{11}{6}} \tag{2}$$

In equation (2), the path length L and wave number k of an optical beam are related to the observed scintillation index through the refractive index structure constant C_n^2. The variance in beam irradiance is measured experimentally using a scintillometer link, with a beam transmitter and receiver separated by a path.

3. Data collection and analysis

To investigate optical turbulence in the low-altitude near-maritime environment, an 890 [m] propagation path was established over the Severn River in Annapolis, Maryland. A scintillometer was used to establish a measure of optical turbulence, C_n^2, with which to compare model predictions. The scintillometer link was approximately 2–3 [m] over the surface of the water depending on tides, with more than 95% of the distance of the propagation path over water. We characterize this propagation environment as 'near-maritime' or 'littoral' with the local atmosphere affected by the land mass on either side of the path [4, 5, 12, 13].

The scintillometer link in figure 1 provided a measure of optical turbulence for the approximately 15-month duration of the study. In addition to collecting measured readings of optical turbulence through C_n^2, a wide variety of local environmental parameters were collected. The choice of local environmental parameters was informed by prior literature [3, 4, 7, 12]. These studies suggested that the air temperature and atmospheric pressure can be used to predict optical turbulence. Further literature suggests that the air water temperature difference, humidity, and wind speed could be useful in predicting C_n^2 [6].

In order to measure these environmental parameters, two local weather stations and a submerged current profiler were deployed next to the receiver of the scintillometer link. Additionally, publicly available data from NOAA was used to supplement hourly-averaged atmospheric and oceanographic readings. More information about each of these data sources and their methodologies is available in [14–18].

The environmental parameters recorded are summarized in table 1 and include both atmospheric and oceanographic features, taken in reasonably close proximity to our scintillometer link. A Scintec BLS450 Large Aperture Scintillometer was used to measure C_n^2 along the path in figure 1 from 01 Jan 2019 until 31 Mar 2020. Hourly averaged data was compiled for the same time range. Additionally, 10 min averaged data was collected

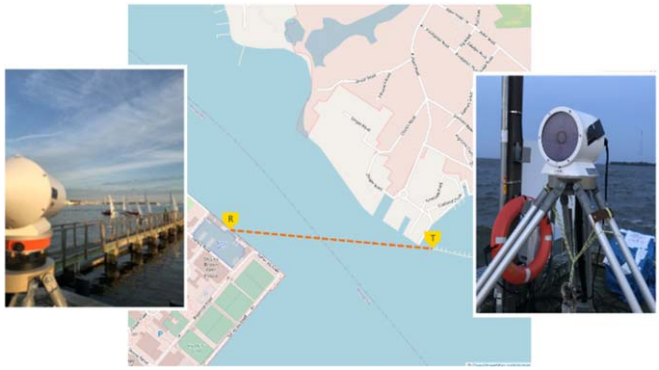

Figure 1. 890 [m] Scintillometer link propagation path [13].

Table 1. Local Environmental parameters with their units and descriptions.

Parameter	Description	Units
C_n^2	The refractive index structure constant C_n^2 describes the extent of optical turbulent effects on beam propagation. It is path dependent, and reported as a path average.	$[m^{-\frac{2}{3}}]$
Air Temperature	Air temperature describes the kinetic energy of the gases which make up the local atmosphere.	[°C]
Relative Humidity	The relative humidity is the ratio of water vapor in the local atmosphere to the maximum possible water vapor content. This parameter is dependent on air temperature.	[%]
Air Pressure	The force of the air column above a local propagation path.	[hPa]
Rain	The height of rain fallen over a 10 min interval.	[cm]
Air-Water Temperature Difference	The difference in temperature between the air and the water below it can describe the extent of turbulent mixing driven by temperature structure function instability.	[°C]
Temporal Hour Weight	The temporal hour weight is a measure of the time elapsed between sunrise and each day's measurement, scaled for the total duration between sunrise and sunset.	—
Seasonality	The seasonality parameter was determined as the fraction of the year which had passed at the time of each observation.	—
Visibility	The distance at which an object can be clearly discerned, measured in nautical miles.	[nm]
Wind Speed	The interval-averaged relative speed of the local wind to a fixed point on the propagation path.	$\left[\frac{m}{s}\right]$
Wind Direction	The direction of interval-averaged mean wind speed measured in degrees true, taken at the same location of wind speed measurements.	[°T]
Solar Radiation	The solar irradiance above the local propagation path.	$\left[\frac{W}{m^2}\right]$
UV Index	A categorical parameter describing the intensity of short-wavelength radiation from the Sun taken alongside the solar radiation, along the propagation path.	—
Air Density	The density of the local atmosphere is related to its pressure and the presence of aerosols. Aerosols include small solid or liquid particles suspended in the air, such as dust or water droplets.	$\left[\frac{g}{m^3}\right]$

between 01 Jan 2019 and 31 Mar 2020. These measurements were split into two data sets based on the frequency of observation [19].

To better visualize the trend in optical turbulence as measured by C_n^2 over the course of one day, a time series of 1 min readings were plotted. Additionally, the performance of two common explicit models, the macro-meteorological model in [5, 12] and the offshore-updated model in [12], were investigated by generating predicted C_n^2 from observed environmental measurements. The equation for the macro-meterological model is given in equation (3) [5, 12].

$$C_n^2 = (3.8 \times 10^{-14})W + f(T) + f(U) + f(RH) - (5.3 \times 10^{-13}),$$

where

$$f(T) = (2.0 \times 10^{-15})T$$

$$f(U) = (-2.5 \times 10^{-15})U + (1.2 \times 10^{-15})U^2 - (8.5 \times 10^{-15})U^3$$

$$f(RH) = (-2.8 \times 10^{-15})RH + (2.9 \times 10^{-17})RH^2 - (1.1 \times 10^{-19})RH^3. \quad (3)$$

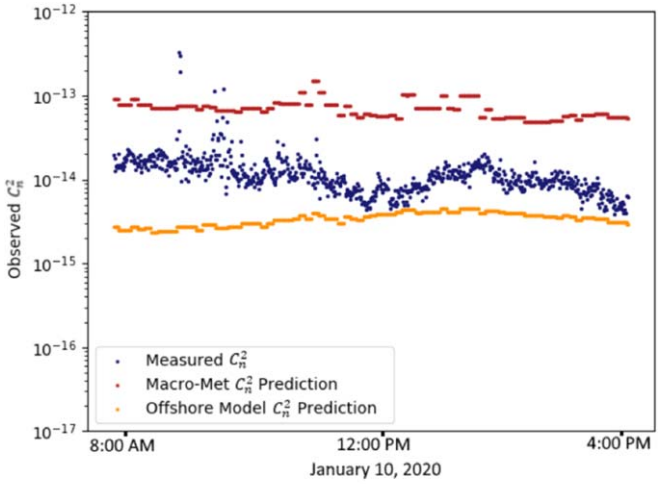

(a)

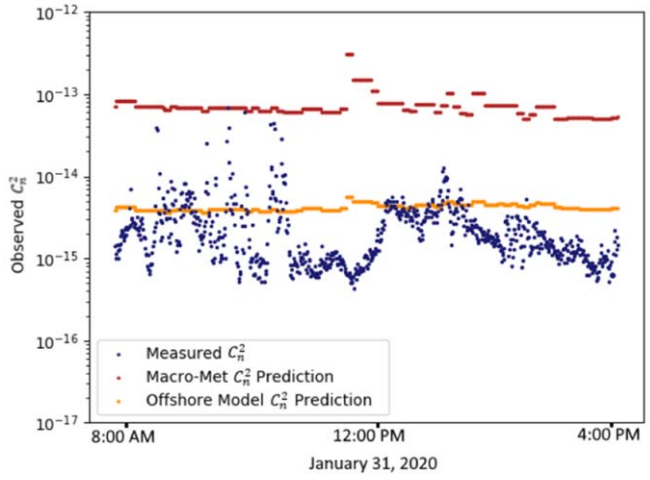

(b)

Figure 2. Comparison between observed and predicted C_n^2 from models in [5, 12] on (a) 10 Jan 2020 and (b) 31 Jan 2020.

The offshore updated model is given in equation (4) [5, 12].

$$C_n^2 = (-1.58 \times 10^{-15})W + f(T) + f(U) + f(RH) - (7.44 \times 10^{-14}),$$

where

$$f(T) = (2.74 \times 10^{-16})T$$

$$f(U) = (3.37 \times 10^{-16})U + (1.92 \times 10^{-16})U^2 - (2.8 \times 10^{-17})U^3$$

$$f(RH) = (8.3 \times 10^{-17})RH - (2.22 \times 10^{-18})RH^2 + (1.42 \times 10^{-20})RH^3. \quad (4)$$

In both equations (3) and (4), W denotes the temporal hour weight, T denotes the tempoerature in $[K]$, RH denotes the relative humidity in [%], and W denotes the wind speed in $\left[\frac{\text{m}}{\text{s}}\right]$. Comparing the predicted C_n^2 with the observed C_n^2 gives insight into the applicability of this model in the near-maritime environment. Two representative days for the 10 min averaged data set, along with the predicted C_n^2 are given in figure 2 [5, 12].

While the macro-meteorological model was reasonable for predicting C_n^2 for the 8 h after sunrise on 10 Jan 2020, there is a general trend towards over- estimation of C_n^2. The mean average error for predicting C_n^2 on 10 Jan 2020 was $7.08 \times 10^{-14}[\text{m}^{-\frac{2}{3}}]$ for the macro-meteorological model and $2.94 \times 10^{-15}[\text{m}^{-\frac{2}{3}}]$ for the offshore update model. For the data on 31 Jan 2020, the macro-meteorological model was far less successful than the offshore updated model, and the over-estimation of optical turbulence is evident. The mean average error for predicting C_n^2 on 31 Jan 2020 was $7.36 \times 10^{-14}[\text{m}^{-\frac{2}{3}}]$ in the macro meterological model, and $1.74 \times 10^{-15}[\text{m}^{-\frac{2}{3}}]$ for the offshore update model. The data suggests that the macro-meteorological model tends to over-predict the extent of near-maritime optical turbulence, especially when measured optical turbulence is below $1 \times 10^{-13}[\text{m}^{-\frac{2}{3}}]$.

Table 2. Dataset measurement summaries for (a) hourly and (b) 10 min averaged data.

	mean	std	min	25%	50%	75%	max
$C_n^2[\mathrm{m}^{-\frac{2}{3}}]$	1.73E-14	3.98E-14	1.02E-16	2.15E-15	6.47E-15	1.63E-14	1.97E-12
Air Temperature [°C]	13.68	8.86	0.00	5.90	10.20	22.80	30.30
Air-Water Temperature Difference [°C]	0.85	3.44	15.00	1.10	0.80	2.90	14.70
Dew Point Temperature [°F]	46	18	10	32	45	62	83
Dry Bulb Temperature [°F]	57	18	12	42	54	73	101
Pressure [*inHg*]	29.96	0.24	29.29	29.74	29.92	30.13	30.76
Pressure Change [*inHg*]	−0.01	0.05	−0.25	−0.05	−0.01	0.02	0.23
Relative Humidity [%]	69	18	14	55	71	83	100
Wet Bulb Temperature [°F]	51.25	15.93	8.00	38.00	49.00	66.00	84.00
Wind Direction [°*T*]	167.50	122.99	0.00	40.00	160.00	300.00	360.00
Gust Wind Speed $[\frac{\mathrm{m}}{\mathrm{s}}]$	21.71	4.39	16.00	18.00	21.00	23.00	57.00
Average Wind Speed $[\frac{\mathrm{m}}{\mathrm{s}}]$	6.80	4.72	0.00	3.00	7.00	10.00	26.00
Visibility [nm]	8.43	2.88	0.00	8.00	10.00	10.00	10.00
Seasonality	0.50	0.29	0.00	0.25	0.50	0.75	1.00
Temporal Hour Weight	0.40	0.60	−0.78	−0.11	0.40	0.90	1.66

(a)

	mean	std	min	25%	50%	75%	max
$C_n^2[\mathrm{m}^{-\frac{2}{3}}]$	2.28E-14	3.05E-14	1.95E-16	5.52E-15	1.21E-14	2.78E-14	3.72E-13
Air Temperature [°C]	7.35	4.69	−4.60	4.20	7.40	10.30	26.60
Air-Water Temperature Difference [°C]	70	20	14	53	71	90	98
Dew Point Temperature [°F]	1.66	6.24	−14.60	−2.80	1.80	6.40	19.80
Dry Bulb Temperature [°F]	1.36	1.08	0.00	0.40	1.30	1.80	6.30
Pressure [*inHg*]	1021	10	982	1014	1021	1028	1044
Pressure Change [*inHg*]	0.00	0.00	0.00	0.00	0.00	0.00	0.00
Relative Humidity [%]	206	213	0	19	129	347	932
Wet Bulb Temperature [°F]	0.74	0.99	0.00	0.00	0.20	1.20	4.80
Wind Direction [°*T*]	1.25	0.03	1.16	1.23	1.25	1.28	1.34
Gust Wind Speed $[\frac{m}{s}]$	3.57	1.67	0.70	1.48	4.77	5.02	5.02
Average Wind Speed $[\frac{m}{s}]$	0.53	0.28	0.00	0.30	0.54	0.77	1.00
Visibility [nm]	−0.02	0.33	−0.68	−0.29	−0.02	0.26	0.59
Seasonality	−2.69	4.88	−15.11	−6.03	−2.74	0.34	15.32
Temporal Hour Weight	0.40	0.60	−0.78	−0.11	0.40	0.90	1.66

(b)

In addition, both the range and distribution of each environmental parameter were consistent with other near-maritime environments in existing literature. After cleaning the data, measurement distributions were computed, as summarized in table 2.

The range and distribution of C_n^2 observations differed slightly month to month, with fatter tails during the spring and fall when rapid temperature and pressure changes occurred. Monthly violin plots of observed $\mathrm{Log}_{10}C_n^2$ are presented in figure 3, along with a histogram for the full data set.

The monthly distributions of observed $\mathrm{Log}_{10}C_n^2$ observations reflect higher than expected optical turbulence for open-ocean link, but are in line with other near-maritime link observations [4, 5]. Existing literature has suggested a relationship may exist between the air water temperature difference and optical turbulence measured as C_n^2. Using these two data sets, the potential physical relationship between air-water temperature difference was investigated. The measured air-water temperature difference is plotted against the $\mathrm{Log}_{10}C_n^2$ in figure 4.

The joint distribution in figure 4 indicates that optical turbulence is higher when the magnitude of air-water temperature difference is high, and typically much lower when the air temperature and water temperature are similar. This may be the result of lower heat flux between the water surface and the layer of atmosphere directly above the surface [1, 4, 5].

4. Conclusions

Near-maritime scintillometer observations collected over the Severn River were analyzed over a period of 15 months from 01 Jan 2019 through 31 Mar 2020. Two representative days for the data set were plotted and compared to two previously published models, the macro meteorological and the offshore update model. The measured optical turbulence was high near local noon, as expected, but did not show as distinct of a diurnal

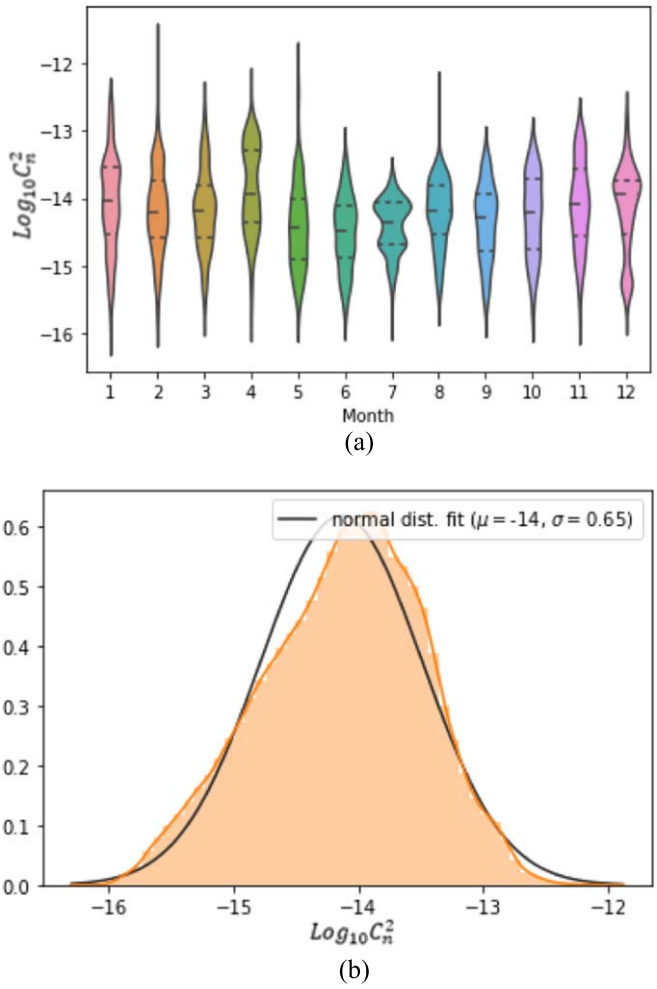

Figure 3. Monthly violin plots (a) and histogram (b) of $Log_{10}C_n^2$ observations.

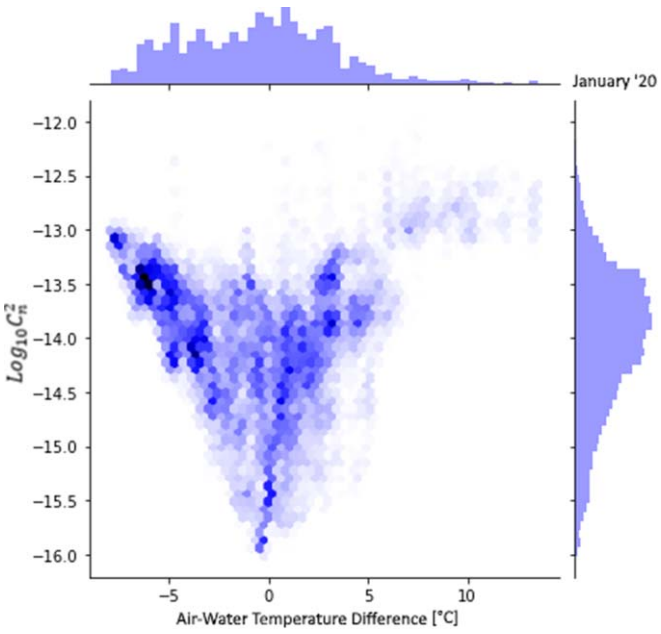

Figure 4. Air-water temperature difference versus $Log_{10}C_n^2$ observations for Jan2020.

trend as is generally associatedfor over-land links [10]. The joint distribution of measured air-water temperature difference against measured $\mathrm{Log}_{10}C_n^2$ for the 15 month hourly-averaged data indicates that optical turbulence was lowest when the air water temperature difference was near 0 [°C]. This trend has been investigated for open-ocean links and some longer near-maritime links [4, 11]. The data collected using the scintillometer link indicates this relationship is present in the near-maritime environment. Explicit models for predicting optical turbulence were applied. The macro-meteorological model was shown to over-estimate C_n^2 in the near-maritime environment, while the offshore-update model showed inconsistency. The data collected in this study suggests that the near-maritime propogation environment is distinct from over-land and open-ocean enviroments. The availability of this data set allows for new models to be developed to improve C_n^2 prediction in a near-maritime environment.

Acknowledgments

The authors thank the USNA technical supprt, ONR, and DEJTO.

Data availability statement

The data that support the findings of this study are openly available at the following URL/DOI:https://github.com/CDJellen/atmospheric-research-repo.

ORCID iDs

Christopher Jellen https://orcid.org/0000-0003-0469-353X

References

[1] Barrios R and Dios F 2012 Wireless optical communications through the turbulent atmosphere: a review Optical Communications Systems, Narottam DasIntechOpen, IntechOpen Limited, London (https://doi.org/10.5772/34740)
[2] Andrews L C and Phillips R L 2005 *Laser Beam Propagation Through Random Media* (Orlando, FL: SPIE) (https://spie.org/Publications/Book/626196?SSO=1) 9780819459480
[3] Frederickson P A, Hammel S and Tsintikidis D 2006 Measurements and modeling of optical turbulence in a maritime environment *Atmospheric Optical Modeling, Measurement, and Simulation II* vol 6303 (San Diego, CA: International Society for Optics and Photonics) p 630307
[4] Mahon R, Moore C I, Burris H R, Rabinovich W S, Stell M and Thomas L M 2009 Analysis of long-term measurements of laser propagation over the Chesapeake Bay *Appl. Opt.* **48** 2388–400
[5] Bourque W, Nelson C and Nelson D 2017 Evidence and implications of differences in atmospheric optical turbulence behavior on opposite coastal environments *Journal of Directed Energy* **6** 187–97
[6] Jellen C, Burkhardt J, Brownell C and Nelson C 2020 Machine learning informed predictor importance measures of environmental parameters in maritime optical turbulence *Appl. Opt.* **59** 6379–89
[7] Tunick A, Tikhonov N, Vorontsov M and Carhart G 2005 *Characterization of Optical Turbulence (Cn2).* (United States: US Army Research Laboratory Adelphi)
[8] Foken T 2006 50 years of the Monin–Obukhov similarity theory *Boundary Layer Meteorol.* **119** 431–47
[9] Högström U L F 1996 Review of some basic characteristics of the atmospheric surface layer *Boundary Layer Meteorol.* **78** 215–46
[10] Tunick A D 1998 *The refractive index structure parameter/atmospheric optical turbulence model: CN2 (No. ARL-TR-1615)* (Adelphi, MD: Army Research Laboratory)
[11] Frederickson P A, Davidson K L, Zeisse C R and Bendall C S 2000 Estimating the refractive index structure parameter over the ocean using bulk methods *J. Appl. Meteorol.* **39** 1770–83
[12] Wang H, Li B, Wu X, Liu C, Hu Z and Xu P 2015 Prediction model of atmospheric refractive index structure parameter in coastal area *J. Mod. Opt.* **62** 1336–46
[13] OpenStreetMaps United States Naval Academy. (n.d.). Retrieved April 17, 2020, through Open Data Commons Open Database License (ODbL)
[14] United States Naval Academy Oceanography Department EDMAPS Online Data Repository. Retrieved April 172020
[15] 2017 Vaisala Weather Transmitter WXT530 Series User Guide. Retrieved April 17, 2020
[16] NOAA National Centers for Environmental Information Station Metadata. (n.d.). Retrieved April 17 2020 from (https://ncdc.noaa.gov/data-access/land-based-station-data/station-metadata)
[17] US Department of Commerce, National Oceanic and Atmospheric Administration, National Weather Service, & National Data Buoy Center. (1996, November 8) National Data Buoy Center Retrieved from (https://ndbc.noaa.gov/measdes.shtm)
[18] NOAA ESRL Improved Sunrise/Sunset Calculator. (n.d.). Retrieved April 17 2020 from (https://esrl.noaa.gov/gmd/grad/solcalc/sunrise.html)
[19] Jellen C 2020 Atmospheric Research RepositoryGitHub repository (https://github.com/CDJellen/atmospheric-research-repo)